OPEN ACCESS Freely available online

PLOS ONE

The Sch9 Kinase Regulates Conidium Size, Stress Responses, and Pathogenesis in *Fusarium graminearum*

Daipeng Chen[1☯], Yang Wang[1☯], Xiaoying Zhou[2], Yulin Wang[1], Jin-Rong Xu[1,2]*

1 State Key Laboratory of Crop Stress Biology for Arid Areas, College of Plant Protection, Northwest A&F University, Yangling, Shaanxi, China, **2** Department of Botany and Plant Pathology, Purdue University, West Lafayette, Indiana, United States of America

Abstract

Fusarium head blight caused by *Fusarium graminearum* is an important disease of wheat and barley worldwide. In a previous study on functional characterization of the *F. graminearum* kinome, one protein kinase gene important for virulence is orthologous to *SCH9* that is functionally related to the cAMP-PKA and TOR pathways in the budding yeast. In this study, we further characterized the functions of *FgSCH9* in *F. graminearum* and its ortholog in *Magnaporthe oryzae*. The Δ*Fgsch9* mutant was slightly reduced in growth rate but significantly reduced in conidiation, DON production, and virulence on wheat heads and corn silks. It had increased tolerance to elevated temperatures but became hypersensitive to oxidative, hyperosmotic, cell wall, and membrane stresses. The Δ*Fgsch9* deletion also had conidium morphology defects and produced smaller conidia. These results suggest that *FgSCH9* is important for stress responses, DON production, conidiogenesis, and pathogenesis in *F. graminearum*. In the rice blast fungus *Magnaporthe oryzae*, the Δ*Mosch9* mutant also was defective in conidiogenesis and pathogenesis. Interestingly, it also produced smaller conidia and appressoria. Taken together, our data indicate that the *SCH9* kinase gene may have a conserved role in regulating conidium size and plant infection in phytopathogenic ascomycetes.

Citation: Chen D, Wang Y, Zhou X, Wang Y, Xu J-R (2014) The Sch9 Kinase Regulates Conidium Size, Stress Responses, and Pathogenesis in *Fusarium graminearum*. PLoS ONE 9(8): e105811. doi:10.1371/journal.pone.0105811

Editor: Richard A. Wilson, University of Nebraska-Lincoln, United States of America

Received June 11, 2014; **Accepted** July 24, 2014; **Published** August 21, 2014

Data Availability: The authors confirm that all data underlying the findings are fully available without restriction. All relevant data are within the paper and its Supporting Information files.

Funding: This work was supported by the National Major Project of Breeding for New Transgenic Organisms (2012ZX08009003) and the National Basic Research Program of China (2012CB114002; 2013CB127703). The funders had no role in study design, data collection and analysis, decision to publish, or preparation of the manuscript.

Competing Interests: The authors have declared that no competing interests exist.

* Email: jinrong@purdue.edu

☯ These authors contributed equally to this work.

Introduction

Fusarium graminearum (teleomorph *Gibberella zeae*) is one of the major causal agents of wheat and barley head blight or scab in North America and other parts of the world [1,2]. It also infects corn and other small grains. Like many other Fusarium species, *F. graminearum* produces several mycotoxins that are harmful to human and animals [3]. Deoxynivalenol (DON) is a trichothecene mycotoxin produced by this pathogen that is of major health concerns and monitored by many governments.

As a potent inhibitor of eukaryotic protein synthesis, DON is also a phytotoxin. In fact, the first virulence gene identified in *F. graminearum* is *TRI5* that encodes the trichodiene synthase essential for DON biosynthesis [4,5]. Since the release of its genome sequence [6], molecular genetics and genomics studies of *F. graminearum* have advanced significantly. Expression profiling studies have identified a variety of genes with different expression levels during plant infection [7,8]. Genes of various biochemical or biological functions have been identified as important virulence or pathogenicity factors in *F. graminearum*, including other genes involved in DON biosynthesis [9,10], components of key signal transduction pathways [11,12,13,14], transcription factors of different DNA-binding domains [15,16,17], and several enzymes required for primary metabolism [18,19,20]. Like many other filamentous ascomycetes, *F. graminearum* has three mitogen-activated protein (MAP) kinase pathways, and all of them play critical roles in pathogenesis and DON production [21,22]. It also has the well-conserved cAMP signaling pathway that is involved in the switching from saprophytic growth to infectious growth [23]. Two genes encoding the catalytic subunits of PKA have distinct and overlapping functions in regulating developmental and plant infection processes in *F. graminearum* [24].

A total of 42 protein kinase genes were found to be important for plant infection by systemic characterization of the *F. graminearum* kinome [21]. One of them, FGSG_00472, is orthologous to *SCH9* of the budding yeast. The Sch9 protein kinase shares sequence similarity with the catalytic subunits of PKA and it is functionally related to cAMP signaling in response to nutrient availability in *Saccharomyces cerevisiae*. It inhibits PKA activity by regulating the localization of Tpk1/2/3 and stability of Tpk2 [25]. Disruption of *SCH9* increases PKA activities [25] and stress tolerance [26]. Similar to mutations in *RAS2* and *CYR1*, down-regulation of glucose signaling by deletion of *SCH9* increases longevity and resistance to oxidative stress and heat shock [27]. In *S. cerevisiae*, SCH9 also is a master regulator of protein synthesis. It is phosphorylated by TORC1 to regulate TORC1-dependent cellular processes, such as ribosome produc-

tion and translation [28,29]. The Sch9 kinase also is involved in the regulation of autophagy together with the TORC1 and cAMP-PKA pathways [30].

Although *SCH9* orthologs are well conserved in plant pathogenic fungi or filamentous ascomycetes, none of them have been functionally characterized. Considering the diverse functions of *SCH9* in *S. cerevisiae* and the importance of cAMP signaling in *F. graminearum*, in this study we further characterized the *Fgsch9* deletion mutant generated in the systemic characterization of the *F. graminearum* kinome [21]. Although it was only slightly reduced in growth rate, the Δ*Fgsch9* mutant was significantly reduced in DON production and virulence. It had increased tolerance to elevated temperatures but increased sensitivities to oxidative, hyperosmotic, cell wall, and membrane stresses. The Δ*Fgsch9* deletion mutant also was defective in conidiogenesis and produced smaller conidia. In the rice blast fungus *Magnaporthe oryzae*, the Δ*Mosch9* deletion mutant also was defective in conidiogenesis and pathogenesis. Interestingly, it also produced smaller conidia and appressoria. These results indicate that the *SCH9* kinase gene may have a conserved role in regulating conidium size and plant infection in plant pathogenic fungi.

Results

Deletion of the *FgSCH9* gene reduces hyphal growth and conidiation

In the functional study of the *F. graminearum* kinome, we noticed that the mutant deleted of FGSG_00472.3 was defective in plant infection [21]. This gene (named *FgSCH9*) encodes a serine/threonine protein kinase that is highly similar to yeast *SCH9*. It is well conserved in filamentous fungi and shares limited homology with MEK kinases of the MAP kinase pathways [31]. In this study, we first confirmed the *Fgsch9* mutant generated in an earlier study [21] by Southern blot analyses. When hybridized with a *FgSCH9* fragment amplified with primers F5 and R6, the wild type had the 4.4-kb *Eco*RI band but the Δ*Fgsch9* mutant SD1 had no hybridization signals. When probed with the *hph* fragment, PH-1 had no hybridization signals. Mutant SD1 had a 2.8-kb band, which is the expected size derived from the gene replacement event (Fig. S1).

The Δ*Fgsch9* mutant was reduced in growth rate and conidiation (Table 1). On PDA agar plates, mutant SD1 produced less aerial hyphae than PH-1 (Fig. 1A). We also noticed that mutant SD1 was reduced in hyphal branching at the edges of colonies formed on 1/2 CM for 36 h in comparison with PH-1 (Fig. 1B). In addition, 70.4±7.9% of the Δ*Fgsch9* conidia had morphological defects. Instead of forming typical Fusarium conidia, the Δ*Fgsch9* mutant produced conidia that lacked foot cells or had fewer septa (Fig. 1C). After measuring 80 conidia per replicate, the average size of the wild-type conidia was estimated to be 47.3±8.3×5.3±0.7 μm (length×width) with measurements from three independent experiments. In the Δ*Fgsch9* mutant strain SD1, conidia had the average size of 38.0±6.1×5.2±0.6 μm, which is approximately 20% smaller than the wild-type conidia. On average, the wild-type conidia had 4.3±0.6 septa after measuring 150 conidia per replicate and repeating three times. The *Fgsch9* mutant produced conidia with 3.1±0.5 septa per conidium.

The Δ*Fgsch9* mutant has increased tolerance to elevated temperatures

To test whether the Δ*Fgsch9* mutant has increased tolerance to elevated temperatures, we assayed germ tube growth after incubation in YEPD for 18 h at 30°C. Similar to incubation at 25°C (Fig. 2A), both PH-1 and Δ*Fgsch9* mutant SD1 germinated and produced germ tubes at 30°C. However, germ tubes of PH-1 often had apical and intercalary swollen bodies when incubated at 30°C but not at 25°C (Fig. 2B). Germ tube growth was normal in the Δ*Fgsch9* mutant SD1 at either 25 or 30°C. These observations suggest that deletion of *FgSCH9* increased tolerance to elevated temperatures, which is similar to what was observed in *S. cerevisiae* [26].

The Δ*Fgsch9* mutant is defective in responses to various environmental stresses

To test whether deletion of *FgSCH9* affects responses to other stresses, we assayed colonial growth of the Δ*Fgsch9* mutant on CM plates with four different chemicals that are representative of oxidative, cell wall, hyperosmotic, and membrane stresses. In comparison with the wild type, mutant SD1 produced significantly smaller colonies after incubation for 3 days in the presence of 0.05% H_2O_2, 300 μg/ml Congo red, 0.7 M NaCl, or 0.01% SDS (Fig. 3A). The Δ*Fgsch9* mutant had restricted hyphal growth, particularly on CM with 0.01% SDS. These results indicated that the Δ*Fgsch9* mutant had increased sensitivities to oxidative, membrane, hyperosmotic, and cell wall stresses. *FgSCH9* must be involved in responses to general environmental stresses in *F. graminearum*. In the budding yeast, the Δ*Fgsch9* mutant has increased sensitivities to oxidative and osmotic stresses [26,32].

To confirm its defects in response to hyperosmotic stress, we assayed conidium germination and germ tube growth in the Δ*Fgsch9* mutant in YEPD with different concentrations of NaCl. After incubation at 25°C for 12 h, germ tube growth was similar between mutant SD1 and PH-1 in the presence of 0.3 M NaCl (Fig. 3B). However, although germination was not inhibited, germ tube growth was significantly reduced by 0.7 M or 1 M NaCl in mutant SD1 but not in PH-1 (Fig. 3B). Therefore, germ tube growth, similar to hyphal growth, is sensitive to hyperosmotic stress in the Δ*Fgsch9* mutant.

New hyphal growth is observed inside dead hyphae of the Δ*Fgsch9* mutant

Interestingly, old hyphae of the Δ*Fgsch9* mutant often had empty, dead intercalary compartments, which may be related to its defects in cell wall integrity. In hyphae from YEPD or PDA cultures, we were able to observe new hyphal growth inside the empty compartments (Fig. 4). Close examination indicated that new hyphal growth emerged through the septal pore area from flanking compartments that were still alive (Fig. 4). These observations indicate that the Δ*Fgsch9* mutant must be able to plug up the septal pore when some hyphal compartments were damaged or became empty. However, this plug up is incomplete or reversible and the Δ*Fgsch9* mutant can re-establish polarized growth through the plugged septal pore area.

The Δ*Fgsch9* mutant is defective in plant infection

To determine the role of *FgSCH9* in pathogenesis, we inoculated flowering wheat heads with conidia from PH-1 and mutant SD1. The spikelets of susceptible wheat cultivar Xiaoyan22 drop-inoculated with the Δ*Fgsch9* mutant still developed typical wheat scab symptoms. However, mutant SD1 was defective in spreading from the inoculated kernels to other spikelets on the same wheat heads. At 14 days post-inoculation (dpi), the average disease index (diseased spikelets per head) was 5.6 for mutant SD1 and 14.7 for PH-1 (Table 1), which was approximately a 62% reduction in virulence. Because it is an important virulence factor [4,5], we also assayed DON production in diseased wheat kernels

Table 1. Phenotypes of the *Fgsch9* mutants in growth, conidiation, pathogenesis, and DON production.

Strain	Growth rate (mm/d)[a]	Conidiation ($\times10^6$/ml)[b]	Disease Index[c]	DON (ppm)[d]
PH-1 (WT)	18.9±0.1[A]*	3.0±0.2[A]	14.7±1.5[A]	1611.5±92.6[A]
SD1 (△*Fgsch9*)	16.2±0.2[B]	1.3±0.3[B]	5.6±1.0[B]	571.1±109.4[B]
SE1	18.5±0.1[A]	2.7±0.2[A]	13.2±0.7[A]	1525.2±86.3[A]
N9 (△*Fgsch9/FgSCH9*)	18.0±0.2[A]	2.4±0.4[A]	14.5±0.6[A]	1593.4±95.9[A]

[a]Daily extension in colony radius on PDA plates.
[b]Conidiation in CMC cultures incubated at 25°C for 5 days.
[c]Diseased spikelets per wheat head at 14 dpi.
[d]DON production in infected wheat kernels harvested from inoculated wheat heads 14 dpi.
*Mean and standard deviation were calculated from four independent replicates. Data were analyzed with the protected Fisher's Least Significant Difference (LSD) test. Different letters were used to mark statistically significant difference (P = 0.05).
doi:10.1371/journal.pone.0105811.t001

harvested at 14 dpi. In comparison with PH-1, the Δ*Fgsch9* mutant also was reduced in DON production (Table 1).

F. graminearum also is a corn pathogen and it can cause Gibberella ear rot and stalk rot. In infection assays with corn silks, both PH-1 and mutant SD1 were able to colonize and cause discoloration. However, the extent of discoloration was significantly reduced in the Δ*Fgsch9* mutant in comparison with the wild type (Fig. 5B). On corn silks inoculated with mutant SD1, discoloration was restricted to the inoculation site. Based on data from three independent experiments, the average discolored region on corn silks inoculated with PH-1 and the *Fgsch9* mutant was 47.6±4.8 mm and 16.7±3.7 mm, respectively. These results further indicate that *FgSCH9* is an important virulence factor in *F. graminearum*.

Expression of *FgSCH9*-GFP fully complemented the defects of mutant SD1

For complementation assays, we generated the *FgSCH9*-GFP fusion construct under its own promoter control and introduced it into the Δ*Fgsch9* mutant SD1. Strain N9 was one of the resulting Δ*Fgsch9/FgSCH9*-GFP transformants identified by PCR assays. It was normal in growth rate, conidiation, and conidium morphology (Fig. 1; Table 1). The defects of mutant SD1 in stress responses and plant infection also were rescued in transformant N9 (Fig. 3; Fig. 5). These results indicate that deletion of *FgSCH9* is directly responsible for all the phenotypes of the Δ*Fgsch9* mutant.

To determine the expression and subcellular localization of FgSCH9 in different growth and developmental stages, we examined GFP signals in transformant N9 by epifluorescence microscopy. In conidia and germ tubes, GFP signals of similar strength were observed in the cytoplasm (Fig. 6). Similar results were obtained in hyphae and ascospores. These data indicate that *FgSCH9* was expressed in all the cell types examined and it had no distinct subcellular localization pattern in *F. graminearum*, which is similar to the localization of Sch9 in *S. cerevisiae* [33].

The *Mosch9* mutant also was reduced in conidium size and virulence

To verify the function of *FgSCH9* in controlling cell size and virulence, we identified its ortholog in the rice blast fungus *M. oryzae*, MGG_14773.6 that was named *MoSCH9* in this study. The *MoSCH9* gene replacement construct was generated by the ligation-PCR approach [34] and transformed into protoplasts of strain Ku80 [35]. The Δ*Mosch9* deletion mutant also was reduced in conidium size (Fig. 7A). Whereas the average size of wild-type conidia was 18.1±1.5×6.0±0.7 μm (length×width), conidia of the Δ*Mosch9* mutant were 15.5±1.7×5.1±0.6 μm. Interestingly,

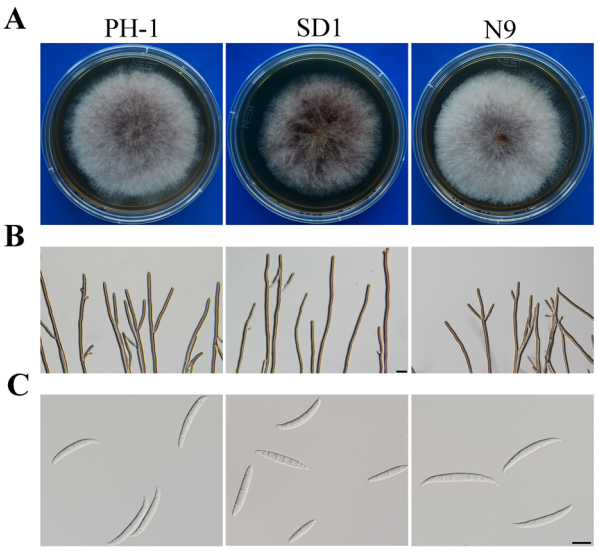

Figure 1. Colony morphology, hyphal growth and conidia morphology. A. Colony morphology of the wild type PH-1, Δ*Fgsch9* mutant SD1, and Δ*Fgsch9/SCH9* transformant N9 cultures grown on PDA. Photographs were taken after incubation for 3 days. **B.** Hyphae of PH-1, SD1, and N9 cultured on 1/2 CM slab agar for 36 h. **C.** Conidia morphology of PH-1, N9, and SD1. Bar = 10 μm.
doi:10.1371/journal.pone.0105811.g001

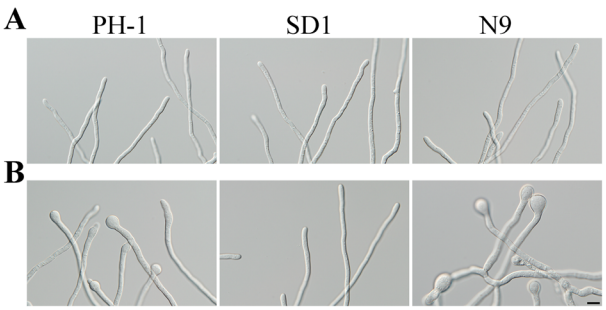

Figure 2. Increased tolerance to elevated temperatures in germ tubes of the Δ*Fgsch9* mutant. Conidia of the wild type PH-1, Δ*Fgsch9* mutant SD1, and Δ*Fgsch9/SCH9* transformant N9 were inoculate in YEPD at 25°C (**A**) and 30°C (**B**). Photographs were taken after incubation for 18 h. Bar = 10 μm.
doi:10.1371/journal.pone.0105811.g002

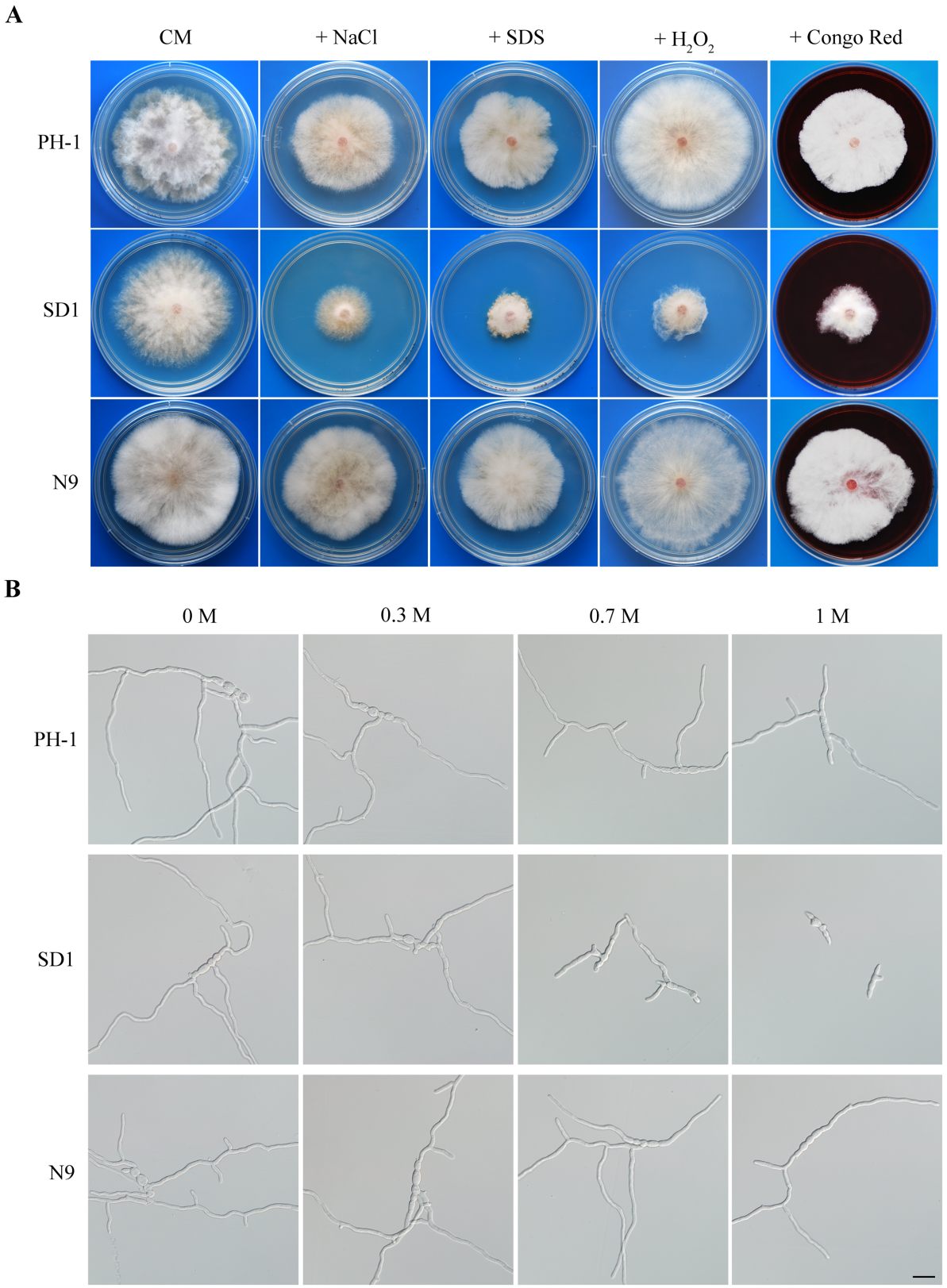

Figure 3. Defects of the Δ*Fgsch9* mutant in response to oxidative, membrane, hyperosmotic, and cell wall stresses. A. Colonies of PH-1, Δ*Fgsch9* (SD1), and complemented transformant N9 cultured on CM plates with 0.05% H_2O_2, 0.7 M NaCl, 0.01% SDS, or 300 μg/ml Congo Red at 25°C for three days. **B.** Conidium germination of PH-1 SD1 and N9 with different concentrantion of NaCl for 12 h. Bar = 20 μm.
doi:10.1371/journal.pone.0105811.g003

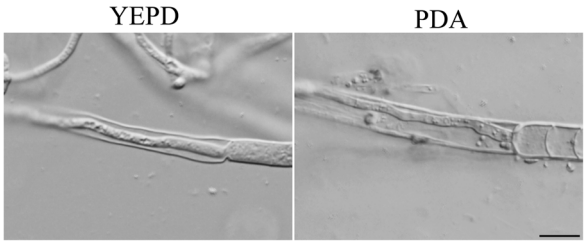

Figure 4. New hyphal growth inside dead compartments in the Δ*Fgsch9* mutant. Hyphae of the Δ*Fgsch9* mutant SD1 grown on YEPD or PDA slab agars were examined by phase contrast microscopy. Bar = 10 μm.
doi:10.1371/journal.pone.0105811.g004

appressoria formed by the Δ*Mosch9* mutant on hydrophobic surfaces also were smaller than those of strain Ku80 (Fig. 7A). On average, the diameter of mutant appressoria was 6.9±0.4 μm. The average size of wild-type appressoria was 8.4±0.5 μm. In infection assays with rice leaves, the Δ*Mosch9* mutant also was reduced in virulence (Fig. 7B). In comparison with Ku80, the mutant produced fewer lesions (Fig. 7B). These results indicate that the *SCH9* orthologs may have conserved functions in regulating cell size and plant infection in fungal pathogens.

Discussion

In the budding yeast, the Sch9 kinase is functionally related to the cAMP-signaling and TORC1 pathways [25,28,30]. These two well-conserved pathways recently were shown to be involved in various development and infection processes in *F. graminearum* [23,24,36]. Although Sch9 orthologs are well conserved in filamentous ascomycetes, none of them have been functionally characterized. In this study, we found that the Δ*Fgsch9* mutant

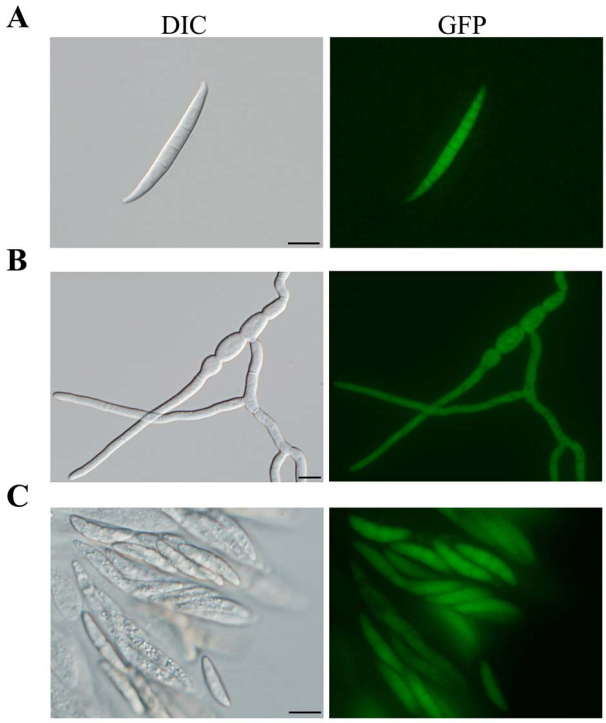

Figure 6. Subcellular localization of FgSch9-GFP fusion proteins. Freshly harvested conidia (**A**), 12 h germlings (**B**), and ascospores (**C**) of the Δ*Fgsch9*/*FgSCH9*-GFP transformant N9 were examined by phase contrast (DIC) or epifluorescence (GFP) microscopy. GFP signals were present mainly in the cytoplasm. Bar = 10 μm.
doi:10.1371/journal.pone.0105811.g006

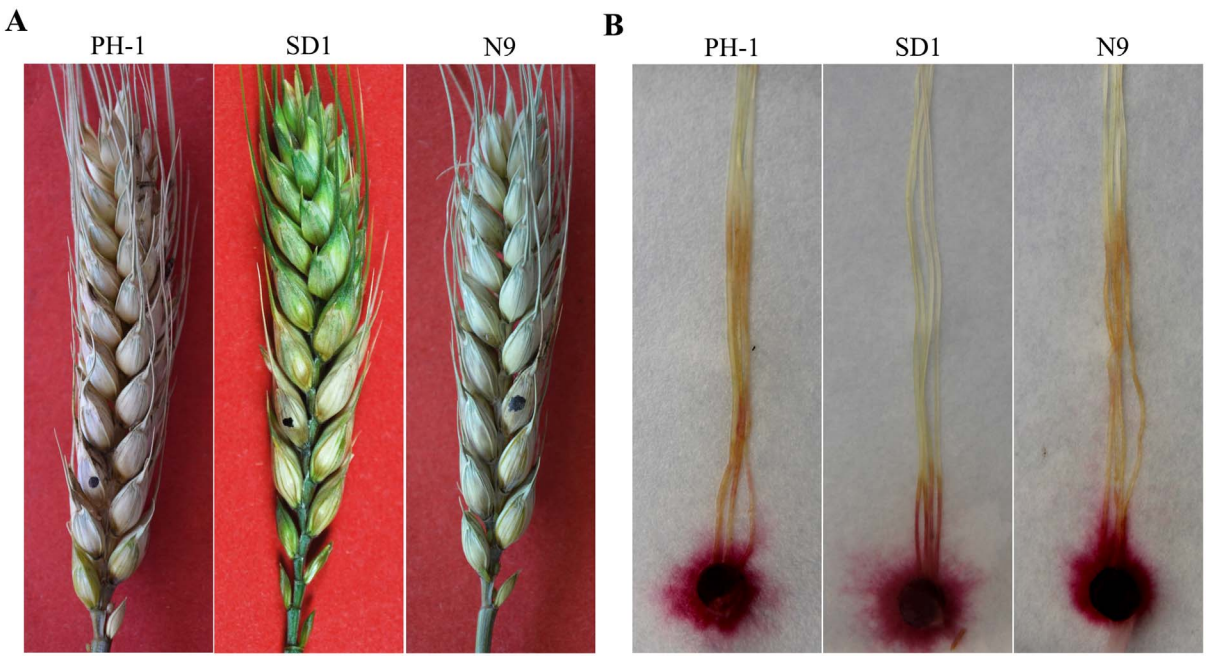

Figure 5. Infection assays with flowering wheat heads and corn silks. A. Flowering wheat heads were drop-inoculated with conidia from the wild type PH-1, Δ*Fgsch9* mutant SD1, and complemented strain N9. Typical wheat heads were photographed 14 dpi. The inoculated kernel was marked with a black dot. **B.** Corn silks were inoculated with culture blocks of the same set of strains and incubated at 25°C. Symptoms were observed at 5 dpi.
doi:10.1371/journal.pone.0105811.g005

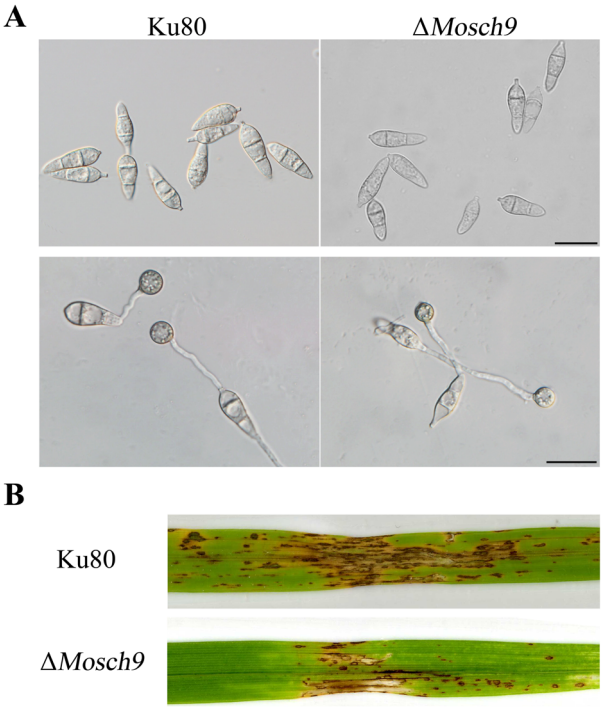

Figure 7. Phenotypes of the Δ*Mosch9* mutant in conidia, appressoria, and pathogenesis. A. Appressorium formation assays with conidia of the wild type Ku80 and the Δ*Mosch9* mutant on hydrophobic plastic coverslips. Typical samples were photographed after incubation at 25°C for 24 h. **B.** Rice leaves wound-inoculated with Ku80 and the Δ*Mosch9* mutant. Lesion formation was observed 7 dpi.
doi:10.1371/journal.pone.0105811.g007

had a reduced growth rate and produced smaller conidia, which is similar to the *sch9* deletion mutant of *S. cerevisiae* that exhibits slow growth and small cell size [33,37,38,39]. In *M. oryzae*, conidia of the Δ*Mosch9* mutant also were smaller than those of the wild type. Even the appressoria produced by the Δ*Mosch9* mutant were smaller. In *C. albicans*, the cell size of the *CaSCH9* deletion mutant was significantly reduced in comparison with that of the wild type strain [40]. Therefore, *SCH9* orthologs may have a conserved function in regulating conidium size in filamentous ascomycetes. In *S. cerevisiae*, *SCH9* and *SFP1* are required for carbon-source modulation of cell size [33].

The TOR complex is well-conserved from yeast to human and it is involved in regulating growth-related signaling. It controls growth in response to nutrients by regulating translation, transcription, ribosome biogenesis, nutrient transport, and autophagy [29,30,41,42]. In *S. cerevisiae*, *SCH9* functions downstream from the TOR pathways for properly regulating ribosome biogenesis, translation initiation, and entry into G_0 phase [28]. In *F. graminearum*, the TOR pathway plays critical roles in regulating vegetative differentiation and virulence [36]. It is likely that *FgSCH9* is also functionally related to the TOR pathway in *F. graminearum*. Unlike *S. cerevisiae* that has *TOR1* and *TOR2*, two TOR kinase genes, *F. graminearum* has a single essential TOR kinase gene [21]. It will be interesting to determine the functional relationship between FgTor1 and FgSch9 by assaying the phosphorylation level or activity of FgSch9 in rapamycin-treated samples.

In the budding yeast, the Sch9 kinase is functionally related to the Ras-cAMP signaling pathway and it shares a large number of phosphorylation targets with PKA, such as Hog1 and Pfk2 [43]. Sch9 inhibits PKA activity and disruption of *SCH9* increases PKA activities [25]. In the fission yeast *Schizosaccharomyces pombe*, Sck1 and Sck2 are homologous to Sch9. Overexpression of the *sck1* or *sck2* gene can suppress the loss of PKA activity [44,45]. *F. graminearum* has only one Sch9 ortholog but two genes encoding catalytic subunits of PKA. Whereas deletion of *CPK2* had no detectable phenotype, the *cpk1* mutant was reduced in growth, virulence, DON production, and conidiogenesis [24]. The *cpk1 cpk2* double mutant had more severe defects in growth and was non-pathogenic [24]. In addition, Sch9 and PKA control parallel pathways that converge on the Rim15 kinase in *S. cerevisiae* [41,46]. In *M. oryzae,* the *rim15* deletion mutant has a slower growth rate, slightly increased sensitivity to hyperosmotic stress, and reduced hyphal melanization and virulence [47]. In *F. graminearum*, the *Fgrim15* mutant was reduced in conidiation and virulence [21].

In *S. cerevisiae*, *SCH9* also is involved in the signal transduction facilitator function of the Hsp90 chaperone complex that is required for the maturation of hundreds of diverse client proteins [48]. The *sch9* mutant has increased stress resistance [26]. In human pathogen *Cryptococcus neoformans*, the *sch9* deletion mutant also had increased thermal tolerance [49]. In *F. graminearum*, the Δ*Fgsch9* mutant had increased tolerance to elevated temperatures during germ tube growth. Germ tubes of the Δ*Fgsch9* mutant were normal but the wild type produced apical and intercalary swollen bodies when incubated at 30°C.

In *F. graminearum*, the Δ*Fgsch9* mutant had increased sensitivity to 0.7 M NaCl, suggesting that *FgSCH9* is important for response to hyperosmotic stress. In the budding yeast, Sch9 is involved in response to hyperosmotic stress via its association with Hog1 and co-regulation of subsets of genes such as *GRE2* and *CTT1* [32]. Nevertheless, the Δ*Fgsch9* mutant had increased sensitivity to SDS and Congo red as well. In addition, we found that the Δ*Fgsch9* mutant had the hyphae-in-hyphae phenotype and increased tolerance to elevated temperatures. Therefore, it is likely that *FgSCH9* is required for general stress responses in *F. graminearum*.

Unlike the *cpk1 cpk2* double mutant [24], the Δ*Fgsch9* mutant was still pathogenic. However, it was significantly reduced in virulence on flowering wheat heads and corn silks. Although *SCH9* orthologs are well-conserved in plant pathogenic fungi or filamentous ascomyctes, none of them have been characterized. However, its ortholog is known to be important for virulence in human pathogens *C. albicans* and *C. neoformans*. The *CaSCH9* deletion mutant was attenuated in virulence in a mouse mode of systemic candidiasis due to its defects in yeast growth and filamentation [40]. In *C. neoformans*, the *SCH9* ortholog functions both independently of and in conjunction with the cAMP-PKA pathway in pathogenesis [49]. In *F. graminearum*, DON is an important virulence factor and the Δ*Fgsch9* mutant was significantly reduced in DON production in infected wheat kernels. In addition, the Δ*Fgsch9* mutant had a reduced growth rate and increased sensitivity to oxidative and other stresses. All these factors may contribute to the defects of the Δ*Fgsch9* mutant in plant infection.

The Δ*Fgsch9* mutant had increased sensitivity to cell wall stresses, indicating defects in cell wall integrity. However, unlike the *mgv1* mutant [22], deletion of *FgSCH9* had no effect on hyphal fusion in *F. graminearum*. Interestingly, old hyphae of the Δ*Fgsch9* mutant often had empty, dead intercalary compartments, likely due to its defects in cell wall integrity. In some of them, new, narrow hyphae were produced from the middle of septa and grew into the empty, dead old hyphae. It appears that the Δ*Fgsch9* mutant can plug up the septal pore when hyphal compartments

become damaged. However, it is defective in this process and somehow can regain polarized growth through the plugged septal pore areas. To our knowledge, this phenomenon of new hyphal growth inside old hyphal compartments has not been reported in *F. graminearum*. Recently, we found that the *tub2* deletion mutant also had similar defects (Zhang and Xu, unpublished). It will be interesting to determine the molecular mechanisms involved in the regulation of septal pore plugging and further growth inside empty hyphal fragments or re-establishment of hyphal tip growth at the septal pore.

Materials and Methods

Strains and culture conditions

The wild-type strain PH-1 and all the transformants of *F. graminearum* generated in this study were routinely cultured on PDA agar plates [50]. Growth rate and conidiation were assayed as described [24,51]. DNA was extracted from vegetative hyphae harvested from liquid YEPD (1% yeast extract, 2% peptone, 2% glucose). Protoplast preparation and PEG-mediated transformation were performed as described [22]. Hygromycin B (Calbiochem, La Jolla, CA) and geneticin (Sigma, St. Louis, MO) were added to the final concentrations of 300 and 350 μg/ml, respectively, to the TB3 medium (0.3% yeast extract, 0.3% casamino acids, 3% glucose) for transformant selection. To test sensitivity against various stresses, vegetative growth was assayed on CM plates with 0.05% H_2O_2, 0.01% SDS, 300 μg/ml Congo Red, or 0.7 M NaCl as described [21,52]. For assaying conidium germination and germ tube growth, conidia were shaken in YEPD (5×10^4 conidia/ml) at 175 rpm for 12 h before examination.

The *M. oryzae* strain Ku80 [35] and transformants generated in this study were cultured on oatmeal agar plates (OTA) as described [53]. Transformants were selected on TB3 with 300 μg/ml zeocin (Invitrogen, Carlsbad, CA) or 250 μg/ml hygromycin B [54].

Generation of *FgSCH9*-GFP fusion constructs and complementation strains

To generate the *SCH9*-GFP fusion constructs, PCR products containing the genomic fragments of the target gene and its promoter sequence were amplified with primers GFPNAT/F and GFPNAT/R (Table S1) and cloned into pFL2 by the yeast gap repair approach [55,56]. The *FgSCH9*-GFP fusion construct was confirmed by sequencing analysis and transformed into protoplasts of the Δ*Fgsch9* mutant. Geneticin-resistant transformants harboring the transforming *FgSCH9*-GFP construct were identified by PCR and confirmed by the presence of GFP signals. The Δ*Fgsch9*/*gSCH9*-GFP complemented transformant N9 was selected for phenotype analysis and subcellular localization analysis of GFP signals.

Infection with *F. graminearum* and DON production assays

For infection assays with flowering wheat heads of cultivars XiaoYan 22 or Norm, conidia were harvested from 5-day-old CMC cultures and re-suspended in sterile distilled water to 2.0×10^5 conidia/ml [57,58]. The fifth spikelet from the base of the spike was inoculated with 10 μl of conidium suspensions as described [59]. Inoculated wheat heads were capped with a plastic bag to maitain humidity for 48 h. After removing the bags, wheat plants were cultured for another 12 days before examination for disease symptoms. The disease index for each strain was estimated by counting diseased spikelets per wheat head at 14 dpi. The inoculated kernels with typical disease symptoms were harvested and assayed for DON production as described [60]. Infection assays with corn silks of cultivar Pioneer 2375 were conducted as described [18]. The extent of discoloration on infected corn silks was measured after incubation at 25°C in a moisture chamber for 5 days [18].

Assays for conidium morphology and size

Conidia were harvested from 5-day-old CMC cultures as described [22] and examined by DIC microscopy. The ones that lacked foot cells or had fewer than four septa were considered to be defective in conidium morphology. For both PH-1 and the *Fgsch9* mutant, conidium morphology assays were repeated three times and 400 conidia were examined in each replicate. To compare their differences in conidium size, the length and width of conidia of PH-1 and the *Fgsch9* mutant were measured in three independent experiments with at least 80 conidia measured per replicate. The average number of septa in conidia was calculated with data from three experiments of counting septa in 150 conidia per replicate. The resulting data were subjected to analyses of variance (ANOVA) with the SPSS17.0 statistics software package (SPSS Inc., Chicago, IL). Comparisons of the means were analyzed with the protected Fisher's Least Significant Difference (LSD) test ($P = 0.05$).

Targeted deletion of the *MoSCH9* gene in *M. oryzae*

To delete the *MoSCH9* gene, its upstream and downstream flanking sequences were amplified with primer pairs MoSCH9-1F/MoSCH9-2R and MoSCH9-3F/MoSCH9-4R, digested with *Fes*I and *Asc*I, respectively. The resulting PCR products were digested and ligated with the hygromycin resistance cassette (*hph*) released from pCX63 as described [34]. The gene replacement construct was amplified with nest primers MoSCH9-1F'/MoSCH9-4R' (Table S1) and directly transformed into protoplasts of Ku80. Hygromycin-resistant transformants were screened by PCR with primers MoSCH9-NF/MoSCH9-NR (Table S1) and confirmed by Southern blot analysis.

Appressorium formation and plant infection with the Δ*Mosch9* mutant

Conidia harvested from 10-day-old oatmeal agar cultures were re-suspended to 10^5 conidia/ml in distilled water for appressorium formation assays on plastic coverslips as described [61,62]. Two-week-old seedlings of rice cultivar CO-39 were used for infection assays with conidia re-suspended 0.25% gelation as described [63]. Disease symptoms were observed 7 dpi.

Supporting Information

Fig. S1 Generation and Southern blot analysis of the Δ*Fgsch9* mutant. **A**. The genomic region of the *FgSCH9* gene and PCR fragments used for generation of the gene replacement construct and Southern blot hybridization. PCR primers were marked with small arrows. E, *Eco*RI. **B**. Southern blots of *Eco*RI-digested genomic DNA of the wild-type strain (PH-1) and Δ*Fgsch9* mutant (SD1) were hybridized with an *FgSCH9* (probe 1) or *hph* fragment (probe 2). Whereas probe 1 hybridized to a 4.4-kb band in PH-1 but not in SD1, probe 2 detected a 2.8-kb band in SD1 that was diagnostic of the gene replacement event.
(TIF)

Table S1 Polymerase chain reaction primers used in this study.
(DOC)

Acknowledgments

We sincerely thank Shijie Zhang and Chaohui Li for helps with wheat and corn silk infection assays. We also thank Tao Yin and Ping Xiang for assistance with DON production assays.

Author Contributions

Conceived and designed the experiments: JRX. Performed the experiments: DPC YW XYZ YLW. Analyzed the data: DPC YW JRX. Contributed reagents/materials/analysis tools: DPC YW XYZ YLW. Contributed to the writing of the manuscript: DPC YW JRX.

References

1. Bai GH, Shaner G (2004) Management and resistance in wheat and barley to Fusarium head blight. Annu Rev Phytopathol 42: 135–161.
2. Goswami RS, Kistler HC (2004) Heading for disaster: *Fusarium graminearum* on cereal crops. Mol Plant Pathol 5: 515–525.
3. Desjardins AE (2003) Gibberella from A (venaceae) to Z (eae). Annu Rev Phytopathol 41: 177–198.
4. Proctor RH, Hohn TM, McCormick SP (1995) Reduced virulence of *Gibberella zeae* caused by disruption of a trichothecene toxin biosynthetic gene. Mol Plant-Microbe Interact 8: 593–601.
5. Harris LJ, Desjardins AE, Plattner RD, Nicholson P, Butler G, et al. (1999) Possible role of trichothecene mycotoxins in virulence of *Fusarium graminearum* on maize. Plant Dis 83: 954–960.
6. Cuomo CA, Gueldener U, Xu JR, Trail F, Turgeon BG, et al. (2007) The *Fusarium graminearum* genome reveals a link between localized polymorphism and pathogen specialization. Science 317: 1400–1402.
7. Zhang XW, Jia LJ, Zhang Y, Jiang G, Li X, et al. (2012) *In planta* stage-specific fungal gene profiling elucidates the molecular strategies of *Fusarium graminearum* growing inside wheat coleoptiles. Plant cell 24: 5159–5176.
8. Boddu J, Cho S, Kruger WM, Muehlbauer GJ (2006) Transcriptome analysis of the barley-*Fusarium graminearum* interaction. Mol Plant-Microbe Interact 19: 407–417.
9. Seong KY, Pasquali M, Zhou X, Song J, Hilburn K, et al. (2009) Global gene regulation by Fusarium transcription factors Tri6 and Tri10 reveals adaptations for toxin biosynthesis. Mol Microbiol 72: 354–367.
10. Menke J, Dong YH, Kistler HC (2012) *Fusarium graminearum* Tri12p influences virulence to wheat and trichothecene accumulation. Mol Plant-Microbe Interact 25: 1408–1418.
11. Jenczmionka NJ, Maier FJ, Losch AP, Schafer W (2003) Mating, conidiation and pathogenicity of *Fusarium graminearum*, the main causal agent of the head-blight disease of wheat, are regulated by the MAP kinase *GPMK1*. Curr Genet 43: 87–95.
12. Urban M, Mott E, Farley T, Hammond-Kosack K (2003) The *Fusarium graminearum* MAP1 gene is essential for pathogenicity and development of perithecia. Mol Plant Pathol 4: 347–359.
13. Nguyen TV, Schafer W, Bormann J (2012) The stress-activated protein kinase FgOS-2 is a key regulator in the life cycle of the cereal pathogen *Fusarium graminearum*. Mol Plant-Microbe Interact 25: 1142–1156.
14. Zheng DW, Zhang SJ, Zhou XY, Wang CF, Xiang P, et al. (2012) The *FgHOG1* pathway regulates hyphal growth, stress responses, and plant infection in *Fusarium graminearum*. Plos One 7: e49495.
15. Son H, Seo Y, Min K, Park A, Lee J, et al. (2011) A phenome-based functional analysis of transcription factors in the cereal head blight fungus, *Fusarium graminearum*. PLoS Pathogens 7: e1002310.
16. Min K, Shin Y, Son H, Lee J, Kim JC, et al. (2012) Functional analyses of the nitrogen regulatory gene *areA* in *Gibberella zeae*. FEMS Microbiol Lett 334: 66–73.
17. Wang Y, Liu W, Hou Z, Wang C, Zhou X, et al. (2011) A novel transcriptional factor important for pathogenesis and ascosporogenesis in *Fusarium graminearum*. Mol Plant-Microbe Interact 24: 118–128.
18. Seong K, Hou ZM, Tracy M, Kistler HC, Xu JR (2005) Random insertional mutagenesis identifies genes associated with virulence in the wheat scab fungus *Fusarium graminearum*. Phytopathology 95: 744–750.
19. Liu X, Wang J, Xu J, Shi J (2014) FgIlv5 is required for branched-chain amino acid biosynthesis and full virulence in *Fusarium graminearum*. Microbiology 160: 692–702.
20. Voigt CA, Schafer W, Salomon S (2005) A secreted lipase of *Fusarium graminearum* is a virulence factor required for infection of cereals. Plant J 42: 364–375.
21. Wang C, Zhang S, Hou R, Zhao Z, Zheng Q, et al. (2011) Functional analysis of the kinome of the wheat scab fungus *Fusarium graminearum*. PLoS Pathogens 7: e1002460.
22. Hou ZM, Xue CY, Peng YL, Katan T, Kistler HC, et al. (2002) A mitogen-activated protein kinase gene (*MGV1*) in *Fusarium graminearum* is required for female fertility, heterokaryon formation, and plant infection. Mol Plant-Microbe Interact 15: 1119–1127.
23. Bormann J, Boenisch MJ, Brueckner E, Firat D, Schaefer W (2014) The adenylyl cyclase plays a regulatory role in the morphogenetic switch from vegetative to pathogenic lifestyle of *Fusarium graminearum* on wheat. PloS One 9: e91135.
24. Hu S, Zhou XY, Gu X, Cao SL, Wang CF, et al. (2014) The cAMP-PKA pathway regulates growth, sexual and asexual differentiation, and pathogenesis in *Fusarium graminearum*. Mol Plant-Microbe Interact 27: In press.
25. Zhang AL, Shen YB, Gao WX, Dong J (2011) Role of Sch9 in regulating Ras-cAMP signal pathway in Saccharomyces cerevisiae. FEBS Lett 585: 3026–3032.
26. Fabrizio P, Pozza F, Pletcher SD, Gendron CM, Longo VD (2001) Regulation of longevity and stress resistance by Sch9 in yeast. Science 292: 288–290.
27. Fabrizio P, Liou LL, Moy VN, Diaspro A, Selverstone VJ, et al. (2003) *SOD2* functions downstream of Sch9 to extend longevity in yeast. Genetics 163: 35–46.
28. Urban J, Soulard A, Huber A, Lippman S, Mukhopadhyay D, et al. (2007) Sch9 is a major target of TORC1 in *Saccharomyces cerevisiae*. Mol Cell 26: 663–674.
29. Huber A, Bodenmiller B, Uotila A, Stahl M, Wanka S, et al. (2009) Characterization of the rapamycin-sensitive phosphoproteome reveals that Sch9 is a central coordinator of protein synthesis. Gene & Dev 23: 1929–1943.
30. Yorimitsu T, Zaman S, Broach JR, Klionsky DJ (2007) Protein kinase A and Sch9 cooperatively regulate induction of autophagy in *Saccharomyces cerevisiae*. Mol Biol Cell 18: 4180–4189.
31. Li G, Zhou X, Xu JR (2012) Genetic control of infection-related development in *Magnaporthe oryzae*. Curr Opin Microbiol 15: 678–684.
32. Pascual-Ahuir A, Proft M (2007) The Sch9 kinase is a chromatin-associated transcriptional activator of osmostress-responsive genes. EMBO J 26: 3098–3108.
33. Jorgensen P, Rupes I, Sharom JR, Schneper L, Broach JR, et al. (2004) A dynamic transcriptional network communicates growth potential to ribosome synthesis and critical cell size. Genes & Dev 18: 2491–2505.
34. Zhao X, Xue C, Kim Y, Xu J (2004) A ligation-PCR approach for generating gene replacement constructs in Magnaporthe grisea. Fungal Genet Newsl 51: 17–18.
35. Villalba F, Collemare J, Landraud P, Lambou K, Brozek V, et al. (2008) Improved gene targeting in *Magnaporthe grisea* by inactivation of *MgKU80* required for non-homologous end joining. Fungal Genet Biol 45: 68–75.
36. Yu F, Gu Q, Yun Y, Yin Y, Xu JR, et al. (2014) The TOR signaling pathway regulates vegetative development and virulence in *Fusarium graminearum*. New Phytologist In press.
37. Geyskens I, Kumara S, Donaton MCV, Bergsma JCT, Thevelein JM, et al. (2000) Expression of mammalian PKB partially complements deletion of the yeast protein kinase Sch9. In: Bos JL, editor. Molecular Mechanisms of Signal Transduction. 117–126.
38. Jorgensen P, Nishikawa JL, Breitkreutz BJ, Tyers M (2002) Systematic identification of pathways that couple cell growth and division in yeast. Science 297: 395–400.
39. Toda T, Cameron S, Sass P, Wigler M (1988) *SCH9*, a gene of *Saccharomyces cerevisiae* that encodes a protein distinct from, but functionally and structurally related to, cAMP-dependent protein-kinase catalytic subunits. Genes & Dev 2: 517–527.
40. Liu W, Zhao J, Li X, Li Y, Jiang LH (2010) The protein kinase CaSch9p is required for the cell growth, filamentation and virulence in the human fungal pathogen *Candida albicans*. FEMS Yeast Res 10: 462–470.
41. Roosen J, Engelen K, Marchal K, Mathys J, Griffioen G, et al. (2005) PKA and Sch9 control a molecular switch important for the proper adaptation to nutrient availability. Mol Microbiol 55: 862–880.
42. Swinnen E, Ghillebert R, Wilms T, Winderickx J (2014) Molecular mechanisms linking the evolutionary conserved TORC1-Sch9 nutrient signalling branch to lifespan regulation in *Saccharomyces cerevisiae*. FEMS Yeast Res 14: 17–32.
43. Zhu G, Spellman PT, Volpe T, Brown PO, Botstein D, et al. (2000) Two yeast forkhead genes regulate the cell cycle and pseudohyphal growth. Nature 406: 90–94.
44. Fujita M, Yamamoto M (1998) *Schizosaccharomyces pombe sck2*(+), a second homologue of *Saccharomyces cerevisiae SCH9* in fission yeast, encodes a putative protein kinase closely related to PKA in function. Curr Genet 33: 248–254.
45. Jin M, Fujita M, Culley BM, Apolinario E, Yamamoto M, et al. (1995) Sck1, a high copy number suppressor of defects in the cAMP-dependent protein-kinase pathway in fission yeast, encodes a protein homologous to the *Saccharomyces cerevisiae* Sch9 kinase. Genetics 140: 457–467.
46. Pedruzzi I, Dubouloz F, Cameroni E, Wanke V, Roosen J, et al. (2003) TOR and PKA signaling pathways converge on the protein kinase Rim15 to control entry into G(0). Mol Cell 12: 1607–1613.
47. Motoyama T, Ochiai N, Morita M, Iida Y, Usami R, et al. (2008) Involvement of putative response regulator genes of the rice blast fungus *Magnaporthe oryzae* in osmotic stress response, fungicide action, and pathogenicity. Curr Genet 54: 185–195.
48. Pearl LH, Prodromou C (2006) Structure and mechanism of the Hsp90 molecular chaperone machinery. Annual Review of Biochemistry 75: 271–294.
49. Wang P, Cox G, Heitman J (2004) A Sch9 protein kinase homologue controlling virulence independently of the cAMP pathway in *Cryptococcus neoformans*. Curr Genet 46: 247–255.
50. Zheng Q, Hou R, Ma J, Wu Z, Wang G, et al. (2013) The MAT Locus Genes Play Different Roles in Sexual Reproduction and Pathogenesis in Fusarium graminearum. PloS one 8: e66980.

51. Zheng Q, Hou R, Zhang JY, Ma JW, Wu ZS, et al. (2013) The *MAT* locus genes play different roles in sexual reproduction and pathogenesis in *Fusarium graminearum*. Plos One 8.
52. Wang G, Wang C, Hou R, Zhou X, Li GH, et al. (2012) The *AMT1* arginine methyltransferase gene is important for plant infection and normal hyphal growth in *Fusarium graminearum*. PLoS One 7: e38324.
53. Xu JR, Hamer JE (1996) MAP kinase and cAMP signaling regulate infection structure formation and pathogenic growth in the rice blast fungus *Magnaporthe grisea*. Genes Dev 10: 2696–2706.
54. Park G, Xue C, Zhao X, Kim Y, Orbach M, et al. (2006) Multiple upstream signals converge on an adaptor protein Mst50 to activate the *PMK1* pathway in *Magnaporthe grisea*. Plant Cell 18: 2822–2835.
55. Bruno KS, Tenjo F, Li L, Hamer JE, Xu JR (2004) Cellular localization and role of kinase activity of *PMK1* in *Magnaporthe grisea*. Eukaryot Cell 3: 1525–1532.
56. Zhou X, Zhang H, Li G, Shaw B, Xu JR (2012) The cyclase-associated potein Cap1 is important for proper regulation of infection-telated morphogenesis in *Magnaporthe oryzae*. PLoS Pathogens 8: e1002911.
57. Ding SL, Mehrabi R, Koten C, Kang ZS, Wei YD, et al. (2009) Transducin beta-like gene *FTL1* is essential for pathogenesis in *Fusarium graminearum*. Eukaryot Cell 8: 867–876.
58. Seong K, Li L, Hou ZM, Tracy M, Kistler HC, et al. (2006) Cryptic promoter activity in the coding region of the HMG-CoA rediactase gene in *Fusarium graminearum*. Fungal Genet Biol 43: 34–41.
59. Gale LR, Chen LF, Hernick CA, Takamura K, Kistler HC (2002) Population analysis of *Fusarium graminearum* from wheat fields in eastern China. Phytopathology 92: 1315–1322.
60. Bluhm BH, Zhao X, Flaherty JE, Xu JR, Dunkle LD (2007) *RAS2* regulates growth and pathogenesis in *Fusarium graminearum*. Mol Plant-Microbe Interact 20: 627–636.
61. Zhou XY, Liu WD, Wang CF, Xu QJ, Wang Y, et al. (2011) A MADS-box transcription factor MoMcm1 is required for male fertility, microconidium production and virulence in *Magnaporthe oryzae*. Mol Microbiol 80: 33–53.
62. Zhao XH, Xu JR (2007) A highly conserved MAPK-docking site in Mst7 is essential for Pmk1 activation in *Magnaporthe grisea*. Mol Microbiol 63: 881–894.
63. Zhao XH, Kim Y, Park G, Xu JR (2005) A mitogen-activated protein kinase cascade regulating infection-related morphogenesis in *Magnaporthe grisea*. Plant Cell 17: 1317–1329.